BRAIN COMMUNICATIONS

Intraepidermal nerve fibre density as biomarker in Charcot–Marie–Tooth disease type 1A

Beate Hartmannsberger,[1] Kathrin Doppler,[1] Julia Stauber,[2] Beate Schlotter-Weigel,[2] Peter Young,[3] Michael W. Sereda[4] and Claudia Sommer[1]

Charcot–Marie–Tooth disease type 1A, caused by a duplication of the gene *peripheral myelin protein 22 kDa*, is the most frequent subtype of hereditary peripheral neuropathy with an estimated prevalence of 1:5000. Patients suffer from sensory deficits, muscle weakness and foot deformities. There is no treatment approved for this disease. Outcome measures in clinical trials were based mainly on clinical features but did not evaluate the actual nerve damage. In our case–control study, we aimed to provide objective and reproducible outcome measures for future clinical trials. We collected skin samples from 48 patients with Charcot–Marie–Tooth type 1A, 7 patients with chronic inflammatory demyelinating polyneuropathy, 16 patients with small fibre neuropathy and 45 healthy controls. To analyse skin innervation, 40-μm cryosections of glabrous skin taken from the lateral index finger were double-labelled by immunofluorescence. The disease severity of patients with Charcot–Marie–Tooth type 1A was assessed by the Charcot–Marie–Tooth neuropathy version 2 score, which ranged from 3 (mild) to 27 (severe) and correlated with age ($P < 0.01$, $R = 0.4$). Intraepidermal nerve fibre density was reduced in patients with Charcot–Marie–Tooth type 1A compared with the healthy control group ($P < 0.01$) and negatively correlated with disease severity ($P < 0.05$, $R = -0.293$). Meissner corpuscle (MC) density correlated negatively with age in patients with Charcot–Marie–Tooth type 1A ($P < 0.01$, $R = -0.45$) but not in healthy controls ($P = 0.07$, $R = 0.28$). The density of Merkel cells was reduced in patients with Charcot–Marie–Tooth type 1A compared with healthy controls ($P < 0.05$). Furthermore, in patients with Charcot–Marie–Tooth type 1A, the fraction of denervated Merkel cells was highly increased and correlated with age ($P < 0.05$, $R = 0.37$). Analysis of nodes of Ranvier revealed shortened paranodes and a reduced fraction of long nodes in patients compared with healthy controls (both $P < 0.001$). Langerhans cell density was increased in chronic inflammatory demyelinating polyneuropathy, but not different in Charcot–Marie–Tooth type 1A compared with healthy controls. Our data suggest that intraepidermal nerve fibre density might be used as an outcome measure in Charcot–Marie–Tooth type 1A disease, as it correlates with disease severity. The densities of Meissner corpuscles and Merkel cells might be an additional tool for the evaluation of the disease progression. Analysis of follow-up biopsies will clarify the effects of Charcot–Marie–Tooth type 1A disease progression on cutaneous innervation.

1 Department of Neurology, University of Würzburg, 97080 Würzburg, Germany
2 Friedrich-Baur-Institute, Department of Neurology, Ludwig-Maximilians-University of Munich, 80336 Munich, Germany
3 Medical Park Bad Feilnbach Reithofpark, Department of Neurology, 83075 Bad Feilnbach, Germany
4 Department of Clinical Neurophysiology, University Medical Center Göttingen (UMG), 37075 Göttingen, Germany

Correspondence to: Claudia Sommer
Department of Neurology,
University of Würzburg, Josef-Schneider-Str. 11, 97080 Würzburg,
Germany
E-mail: sommer@uni-wuerzburg.de

Received October 24, 2019. Revised January 08, 2020. Accepted January 24, 2020. Advance Access publication February 12, 2020

Keywords: Charcot–Marie–Tooth disease type 1A; skin punch biopsy; intraepidermal nerve fibre density; Merkel cell density; reproducible outcome measure

Abbreviations: CIDP = chronic inflammatory demyelinating polyradiculoneuropathy; CMT = Charcot–Marie–Tooth disease; CMT1A = Charcot–Marie–Tooth disease type 1A; CMTNS = CMT neuropathy score;CMTNSv2 = Charcot–Marie–Tooth neuropathy score version 2; IENFD = intraepidermal nerve fibre density; IENFs = intraepidermal nerve fibres; ONLS = overall neuropathy limitation scale; PGP9.5 = protein gene product 9.5; PMP22 = peripheral myelin protein 22 kDa; SFN = small fibre neuropathy

Graphical Abstract

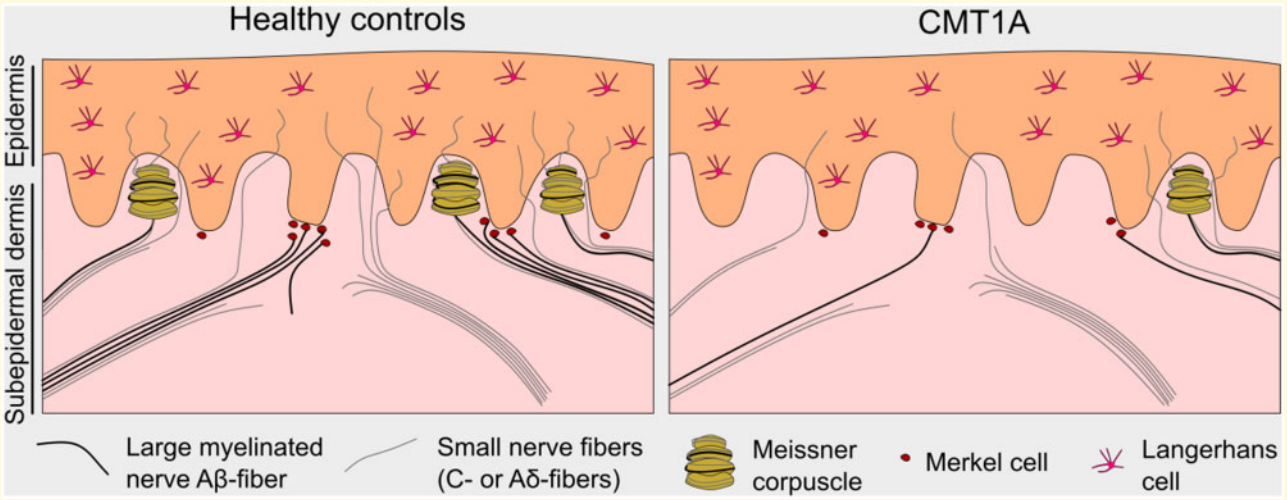

Introduction

Charcot–Marie–Tooth (CMT) disease is the most prevalent hereditary motor and sensory peripheral neuropathy (Barreto *et al.*, 2016). The most common subtype is CMT type 1A (CMT1A) with an estimated frequency of 1:5000 (Gess *et al.*, 2013; Manganelli *et al.*, 2014), caused by an autosomal-dominantly transmitted duplication of the gene *peripheral myelin protein 22 kDa* (*PMP22*) on chromosome 17p11.2, which encodes for PMP22 (Li *et al.*, 2013). The 1.5-fold overexpression of PMP22 (Lee *et al.*, 2018), one of the main myelin proteins (Snipes and Suter, 1995), causes demyelination, which leads to length-dependent axonal degeneration and reduced nerve conduction velocity (Pareyson *et al.*, 2006). CMT1A disease usually starts in childhood, and patients predominantly suffer from muscle weakness and wasting, mostly in the lower limbs, which can lead to foot deformities (Pareyson *et al.*, 2006) and in some cases even wheelchair dependency (Van Paassen *et al.*, 2014).

Currently, there is no treatment approved for CMT1A. There have been clinical trials testing ascorbic acid (Micallef *et al.*, 2009; Pareyson *et al.*, 2011; Lewis *et al.*, 2013; Gess *et al.*, 2015), all of which unfortunately showed no beneficial clinical effects. Treatment with the triplet medication PXT3003 (baclofen, naltrexone and sorbitol) had a mild benefit over placebo (Attarian *et al.*, 2014). All these studies measured the effects primarily by comparing clinical scores such as the CMT neuropathy score (CMTNS) or the overall neuropathy limitation scale as primary outcome measure, which evaluate impairment, physical limitations and electrophysiology (Reilly *et al.*, 2010; Wang *et al.*, 2017). However, the sensitivity of CMTNS as an outcome measure has been critically discussed (Wang *et al.*, 2017) leading to further adaptation to the CMTNS version 2 (CMTNSv2) (Murphy *et al.*, 2011) and to suggestions for secondary outcome measures, e. g. foot dorsal flexion or 9 hole-peg test (Mannil *et al.*, 2014). Cutaneous expression of several genes has been proposed as additional disease severity and progression marker in patients with CMT1A (Fledrich *et al.*, 2017).

Although these neuropathy score measures for the evaluation of the CMT severity are extensive, they only provide information about clinical and functional parameters, but the actual nerve damage is not assessed. Thus, it is very important to find additional biomarkers that will provide objective and reproducible outcome criteria assessing the actual nerve damage for future clinical trials in CMT1A.

Nerve fibres in the dermis are usually part of nerve bundles, which consist of unmyelinated fibres only or of both myelinated and unmyelinated fibres. Unlike unmyelinated C-fibres and thinly myelinated Aδ-fibres, large

myelinated Aβ-fibres do not terminate in the epidermis as free nerve endings but innervate mechanoreceptors such as Meissner corpuscles and Merkel cells. Small calibre C- and Aδ-fibres penetrate the epidermis and terminate there as free nerve endings, which are called intraepidermal nerve fibres (IENFs). We could previously show that the dermal nerve bundle density is a sensitive measure in peripheral neuropathies (Doppler *et al.*, 2012). A previous study suggested myelinated fibre morphology in finger biopsies from patients with CMT1A for the evaluation of nerve damage (Li *et al.*, 2005).

Meissner corpuscles are mechanoreceptors, which consist of an inner bulb formed by Schwann cells, enwrapped by up to three large myelinated fibres and up to two unmyelinated C-fibres (Abraira and Ginty, 2013). They are located in the dermal papillae of glabrous skin. Decreased Meissner corpuscle density has previously been reported in skin biopsies from the finger tip of patients with CMT1A compared with controls in a smaller cohort (Nolano *et al.*, 2015). Another mechanoreceptor type, the Merkel cells, is located at the epidermal–dermal junction. They are usually in close contact with unmyelinated nerve endings derived from large myelinated Aβ-fibres and form the so-called 'touch spots' (Boulais and Misery, 2007). Merkel cell survival is dependent on their innervation by myelinated axons (Airaksinen *et al.*, 1996). To our knowledge, Merkel cell density has not been assessed in patients with CMT1A. In mouse models deficient for P0, Merkel cell density was shown to be reduced in glabrous and hairy skin compared with wild-type mice (Frei *et al.*, 1999).

Skin punch biopsy has proved an important minimally invasive tool for the assessment of cutaneous innervation in patients with various neuropathy (Sommer, 2008; Lauria *et al.*, 2009; Doppler *et al.*, 2013), e.g. diabetic neuropathy or small fibre neuropathies (SFN) (Sommer, 2018). A well-established measure in the skin is the IENF density (IENFD), which can be assessed by immunostaining.

In healthy subjects, IENFD is known to decrease with age, whereas women have higher IENFDs compared with men of the same age (Collongues *et al.*, 2018). In previous studies, IENFD has consistently been reported to be decreased in biopsies from the distal leg or the fingertips in CMT1A (Nolano *et al.*, 2015; Duchesne *et al.*, 2018).

Several previous studies provided evidence that the investigation of nerve fibres in skin biopsies from patients with CMT1A may be useful (Li *et al.*, 2005; Saporta *et al.*, 2009; Manganelli *et al.*, 2015; Nolano *et al.*, 2015) but only analysed single parameters mostly in small cohorts. Larger studies investigating a wider range of parameters are needed to establish skin biopsies as a potential outcome measure for clinical studies.

In this study, we provide an extensive analysis of numerous parameters regarding the cutaneous innervation (IENFD, dermal nerve bundles, mechanoreceptor densities) and nodal architecture of biopsy specimens from the glabrous skin from a cohort of 48 patients with CMT1A in comparison with 7 patients with chronic inflammatory demyelinating polyradiculoneuropathy (CIDP), 16 patients with SFN and 45 healthy controls using immunostaining, to obtain objective and reproducible outcome criteria for future clinical trials.

Materials and methods

Patients

Adult patients with a genetically confirmed diagnosis of CMT1A without any other neurological diseases were recruited for the CMT-NET study in the hospitals of Münster, München, or Göttingen (inclusion criteria: clinical diagnosis of CMT1A, genetic confirmation of CMT1A, age between 18 and 65 years, ability to accomplish the outcome measures at baseline and signed informed patient consent; exclusion criteria: pregnancy/nursing, relevant neurological, psychiatric or internistic disorders, drug or alcohol addiction, permanent vitamin C intake and participation in an interventional clinical study 4 weeks before enrolment). The 3-mm skin punch biopsies were taken from healthy controls and patients with CIDP, SFN and CMT1A from the lateral, glabrous part of the index finger as previously described (Li *et al.*, 2005). Samples from patients with CIDP and SFN and healthy controls had already been collected for previous studies at the University Hospital of Würzburg (Doppler *et al.*, 2018; Üçeyler *et al.*, 2018). Only half of the 3-mm skin biopsies from patients with CMT1A were used for immunostaining.

The CMTNSv2 was used for disease severity evaluation. It is composed of nine items, assessing motor and sensory symptoms, each of which is rated from 0 (none) to 4 (maximum) (Murphy *et al.*, 2011). The subscores are sensory symptoms, motor symptoms (legs), motor symptoms (arms), pinprick sensibility, vibration, strength (legs), strength (arms), ulnar CMAP and radial SNAP amplitude.

Written informed consent was obtained from all patients. The ethics committees of the universities München, Münster and Göttingen approved the study (IRB number: 31-2-16).

Immunostaining

Skin biopsy specimens (only half specimens from patients with CMT1A because the other half is used for separate analyses within the consortium) were fixed in 4% paraformaldehyde for 30 min and stored in 10% sucrose for shipment until freezing. Cryopreserved samples were cut into 40-µm sections and double-immunolabelled with anti-protein gene product 9.5 (PGP9.5, Product Code: 7863-1004, 1:200; Bio-Rad, Hercules, CA, USA; or Cat. No. 516-3344, 1:200; Zytomed Systems, Berlin,

Germany), anti-MBP (Cat. No. GTX11159, 1:200; GeneTex, Irvine, CA, USA), anti-cytokeratin20 (Cat. No. 61054, 1:40; PROGEN Biotechnik, Heidelberg, Germany), anti-S-100 (Cat. No. ab868, 1:100; Abcam, Cambridge, UK), anti-pan-sodium channel (Product No. S8809, 1:100; Sigma Aldrich, St. Louis, MO, USA), anti-Caspr (Cat. No. ab34151, 1:500; Abcam), anti-neurofascin-155 (Cat. No. ab31457, 1:100; Abcam) or anti-Langerin/CD207 (Cat. No. DDX0362, 1:500; Dendritics, Lyon, France). Incubation of sections with primary antibodies was performed overnight at 4°C, and incubation with suitable secondary antibodies (Cy3-conjugated anti-mouse IgG, Cat. No. 715-165-151, 1:100; Jackson ImmunoResearch, Suffolk, Great Britain; Alexa Fluor488-conjugated anti-rabbit IgG, Cat. No. 711-545-152, 1:400; Jackson ImmunoResearch) was performed at room temperature for 2 h. For mounting the sections, VECTASHIELD Mounting Medium with 4′,6-Diamidin-2-phenylindol was used (Vector Laboratories Inc., Burlingame, CA, USA).

Microscopy

A fluorescence microscope (Zeiss Axiophot 1; Zeiss, Oberkochen, Germany) with an Axiocam MRm camera (Zeiss) and SPOT software (Diagnostic Instruments, Sterling Heights, MI, USA) was used for the image acquisition of epidermis and dermis necessary for density determinations of IENFD, nerve bundles, Merkel cells and Langerhans cells with a 2.5× objective. Linear measurements of nodal and paranodal lengths were done with a 40× objective. Epidermis lengths and dermis areas were measured manually using ImageJ. Counting of IENFs, nerve bundles, Merkel cells, Meissner corpuscles and Langerhans cells was done using a fluorescence microscope Ax10 (Zeiss). The investigator was blinded for the evaluation by pseudonymization of the specimens.

For the analysis of IENFs, sections were double-labelled with anti-PGP9.5 combined with anti-MBP and anti-CK20. In total, the entire epidermis length of 4–6 sections (3–17.8 µm) was analysed per sample. Nerve fibres were counted as described elsewhere (Lauria *et al.*, 2005). For the assessment of the density of bundles with and without myelinated fibres, sections were double-labelled with anti-PGP9.5 and anti-MBP. The numbers of nerve bundles in the dermis of 2–3 sections per sample (bundle with >5 fibres) were counted, and the area of the whole dermis was determined per section. Samples yielding <0.5 mm^2 in total dermis area were excluded from the analysis, which provided us with 46 CMT1A, 7 CIDP, 15 SFN and 41 control samples. Meissner corpuscle density was determined by counting the numbers of papillae and Meissner corpuscles of the entire epidermis of 3–6 sections (16–168 papillae) double-labelled with anti-S100/-PGP9.5 and anti-MBP/-PGP9.5. To determine the Merkel cell density, we counted the numbers of innervated and denervated Merkel cells at the whole epidermal–dermal junction of 2–3 sections (1.4–8.8 mm) double-labelled with anti-CK20 and anti-PGP9.5. Epidermal length was measured, and Merkel cell density of both innervated and denervated cells was expressed as Merkel cells/mm. When possible, five randomly selected nodes from 1–3 sections per sample were analysed regarding the axonal diameter, nodal and paranodal lengths for analysis of the nodes of Ranvier. A total of 164 nodes from 43 CMT1A samples, 34 nodes from seven CIDP samples, 75 nodes from 15 SFN samples and 189 nodes from 42 control samples were analysed. The asymmetry index was calculated as previously described (Saporta *et al.*, 2009), and the ratio of nodal length to diameter was calculated. Nodes that showed a length-to-diameter ratio of >1 were considered long. Langerhans cell density was determined by counting the numbers of Langerhans cells in 2–3 sections per sample (1.3–9 mm) and measuring the length of the epidermis. Langerhans cell density was expressed as Langerhans cells/mm.

Statistical analysis

Statistical analyses were performed using the Python library *SciPy* version 1.2.1 in Python version 3.7.3 (Python Software Foundation, Delaware, USA). To test whether data sets were normally distributed, Shapiro–Wilk test for normality was performed. For comparison, two-tailed Mann–Whitney *U* tests were performed. For correlation analyses, Pearson correlation coefficients were calculated. Binomial tests were performed for the comparison of fractions of long nodes in the analysis of nodes of Ranvier. For $P < 0.05$, differences were considered statistically significant.

Data availability statement

Anonymized data are available from the corresponding author upon reasonable request.

Results

Patients

Demographic and basic clinical data are given in Table 1. Disease severity of the 48 patients with CMT1A ranged from mild to severe and correlated positively with age ($R = 0.402$, $P < 0.005$, Fig. 1). Although the CMT1A group was significantly younger than the 45 subjects from the healthy control group, this difference was small. For comparisons with classic demyelinating and axonal neuropathy groups, biopsies from 7 patients with CIDP and 16 patients with SFN were included. Age and sex distribution of the SFN group were comparable to the CMT1A group, whereas the age of the CIDP group was clearly higher due to the late onset of CIDP (Table 1).

Table 1 Demographic and skin biopsy data

Medians (range)	CMT1A, n = 48	CIDP, n = 7	SFN, n = 16	Controls, n = 45	Ranksums, CMT1A–control
Age (years)	47 (21–63)	60 (43–76)	51 (31–63)	54 (22–64)	**$P < 0.05$**
Sex (male:female)	20:28	6:1	6:10	21:24	–
CMTNSv2	18 (3–27)	–	–	–	–
IENFD (1/mm)	3.7 (0.0–17.3)	6.1 (2.7–7.5)	5.85 (0.3–15.3)	5 (0.8–24.9)	**$P < 0.01$**
Merkel cell density (1/mm)	0.50 (0–3.5)	0.10 (0–6.5)	1.05 (0–6.7)	1.10 (0–11.1)	**$P < 0.05$**
Fraction of denervated Merkel cells (CMT1A: 39, CIDP: 5, SFN: 12, control: 40)	0.80 (0–1)	0.30 (0–1)	0.30 (0–0.7)	0.20 (0–1)	**$P < 0.01$**
Meissner corpuscle density (1/papilla)	0.037 (0–0.154)	0.029 (0–0.153)	0.042 (0.012–0.137)	0.053 (0–0.171)	$P = 0.06$
Density of bundles with (1/mm^2) (CMT1A: 46, CIDP: 7, SFN: 15, control: 41)	4.7 (0–11.7)	2.6 (0.5–5.3)	1.9 (0–5.0)	2.4 (0–12.2)	**$P < 0.01$**
Density of bundles without (1/mm^2) (CMT1A: 46, CIDP: 7, SFN: 15, control: 41)	1.35 (0–6.3)	1.60 (0–6.2)	1.60 (0–5.1)	1.30 (0–6.0)	$P = 0.7$
Node numbers	164	34	75	189	–
Axonal diameter (μm)	1.48 (0.56–3.7)	1.38 (0.74–3.7)	1.67 (0.56–3.7)	1.48 (0.74–4.81)	$P = 0.08$
Node length (μm)	1.1 (0.37–2.96)	1.5 (0.56–12.95)	1.3 (0.56–4.26)	1.3 (0.56–4.81)	**$P < 1 \times 10^{-8}$**
Paranode length (μm)	8.3 (3.1–16.6)	9.7 (5.7–22.6)	8.5 (4.8–47.9)	9.1 (5.4–22.4)	**$P < 0.001$**
Asymmetry index (%)	14 (0–100)	11.8 (0–44.8)	11.1 (0–82.8)	12.35 (0–100)	$P = 0.5$
Ratio node length/diameter	0.70 (0.2–2.2)	0.84 (0.42–11.67)	0.78 (0.2–3.33)	0.80 (0.23–6.5)	**$P < 1 \times 10^{-4}$**
Fraction of long nodes	9.8%	38.2%	37.3%	25.4%	Binomial test: **$P < 1 \times 10^{-6}$**
Langerhans cell density (1/mm) (control: 44)	10.0 (2.5–37.6)	14.6 (8.3–28.5)	8.4 (6.0–20.6)	9.9 (1.3–131.2)	$P = 0.4$

Note: *P*-values smaller than 0.05 are bold.

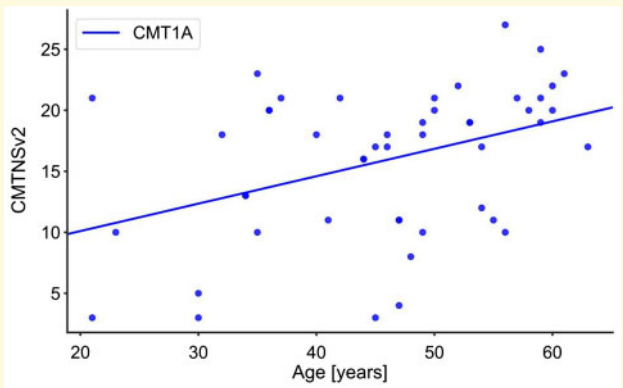

Figure 1 Correlation between age and CMTNSv2 in patients with CMT1A ($P < 0.005$, $R = 0.402$).

Intraepidermal nerve fibre density

The IENFD of patients with CMT1A was significantly decreased compared with the healthy control group (Fig. 2A and Table 1). Representative images of sections from a healthy control and a patient with CMT1A are shown in Fig. 2E and F. In addition, IENFD had a trend to be lower in males compared with females in both CMT1A and the control groups (Fig. 2B), which is in accordance with the literature (Gøransson *et al.*, 2004; Duchesne *et al.*, 2018). When analysed by sex, both the male and female CMT1A groups showed reduced IENFD compared with the male and female control groups, respectively (Fig. 2B). Separate correlation analyses by sex were not performed due to relatively small cohort sizes ($n = 20$–28). The IENFD of the control group showed inverse correlation with age ($R = -0.51$, $P < 0.0005$, Fig. 2C). Interestingly, in our CMT1A cohort, IENFD did not correlate with age ($R = -0.22$, $P = 0.13$, Fig. 2C) but correlated inversely with the CMTNSv2 score ($R = -0.29$, $P < 0.05$, Fig. 2D). When analysing the single subscores, there was a negative correlation of IENFD with the leg strength score ($R = -0.33$, $P < 0.05$). Since biopsies from patients with CMT1A were only half the size of the biopsies from the other groups, we checked if the length of the analysed epidermis had an influence on the IENFD results of the CMT1A and control groups. In fact, the length of the analysed epidermis did not correlate with the assessed IENFD of both groups (control: $R = 0.08$, $P = 0.6$; CMT1A: $R = 0.13$, $P = 0.4$; Supplementary Fig. 1).

Taken together, these aspects suggest that the IENFD might be a candidate for a possible outcome measure in CMT1A.

Bundle densities

The density of bundles without myelinated nerve fibres did not differ between the groups (Fig. 3A). Surprisingly, the density of bundles with myelinated nerve fibres was significantly higher in the CMT1A group compared with the SFN and control groups (Fig. 3B). Representative micrographs are shown in Fig. 3C and D. Thus, we also checked for dermis area dependence of the bundle densities. Indeed, the density of bundles with myelinated fibres correlated negatively with the analysed dermis area in both groups (control: $R = -0.276$, $P = 0.08$, CMT1A: $R = -0.414$, $P < 0.005$; Supplementary Fig. 2A), whereas

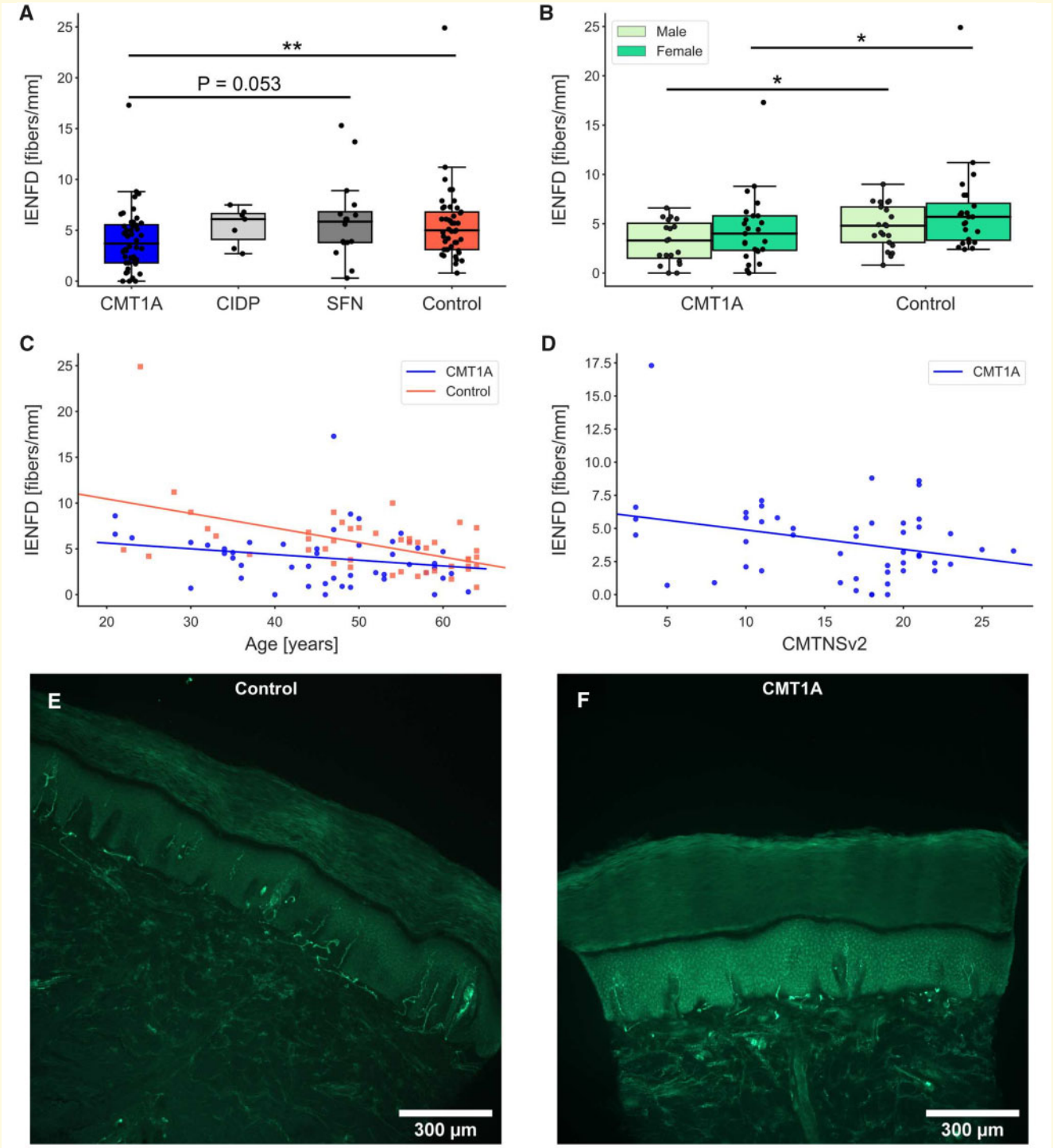

Figure 2 IENFD in patients with CMT1A compared with CIDP, SFN and healthy controls. (**A**) There was a significant reduction in IENFD in CMT1A compared with the healthy control group; $^{**}P < 0.01$. (**B**) In CMT1A and controls, IENFD of females showed a trend to be higher compared with the IENFD of men of the same group (n.s.). Significant differences were still present between CMT1A and controls when divided into males and females; $^{*}P < 0.05$. (**C**) In controls, IENFD showed an inverse correlation with age ($P < 0.001$, $R = -0.51$), but not in patients with CMT1A ($P = 0.1$, $R = -0.22$). (**D**) In CMT1A, IENFD correlated negatively with the CMTNSv2 ($P < 0.05$, $R = -0.29$). Representative micrographs of skin sections labelled with anti-PGP9.5 from a control (**E**) and a patient with CMT1A (**F**). The control section shows a higher IENFD than the CMT1A section.

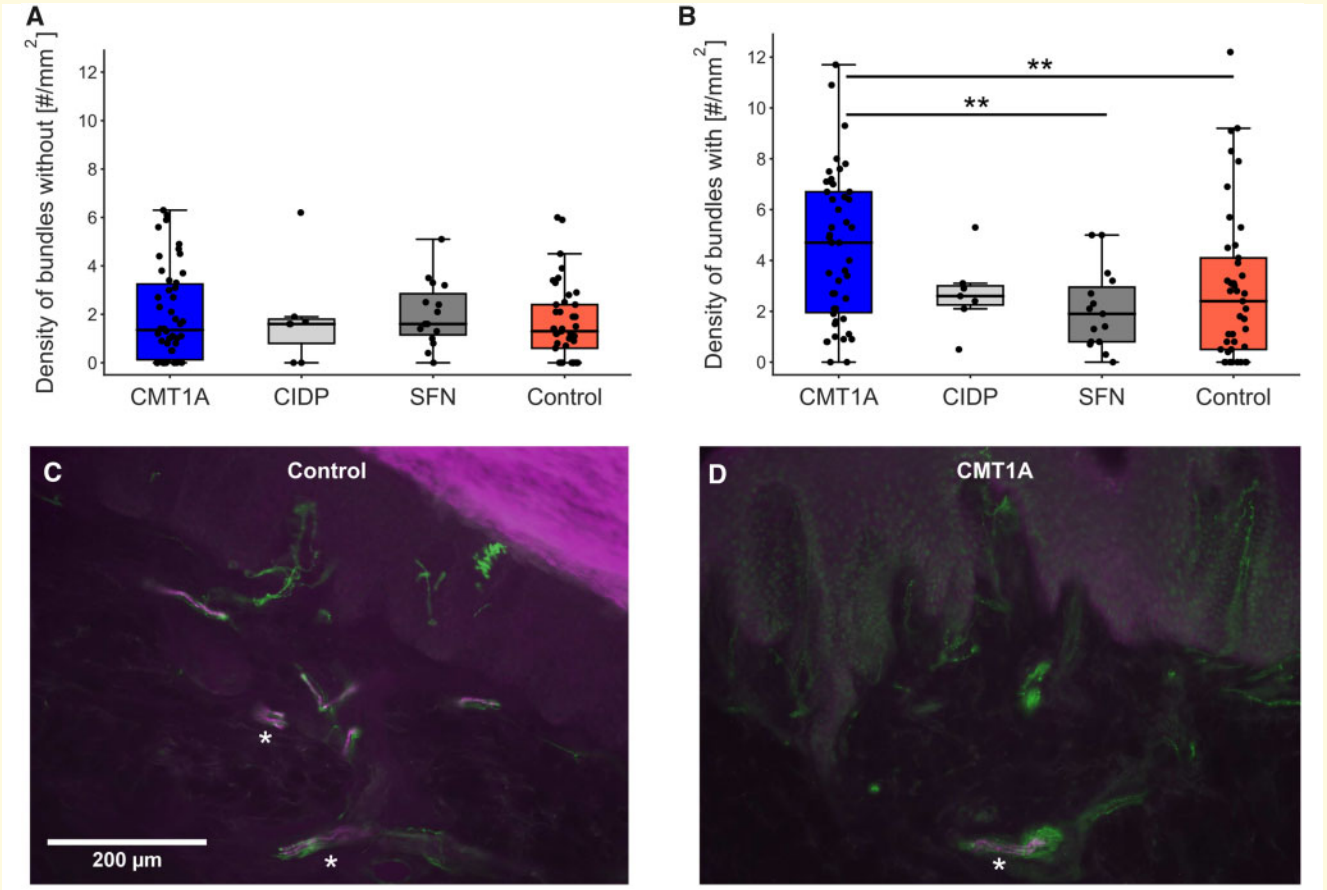

Figure 3 Density of bundles without (A) and with (B) myelinated fibres. (A) There were no significant differences in the bundle densities without myelinated nerve fibres between the groups. (**B**) Elevated density of bundles with myelinated fibres in patients with CMT1A compared with SFN and control groups; $^{**}P < 0.01$. Micrographs of sections stained with anti-PGP9.5 (green) and anti-MBP (magenta) to illustrate nerve fibre bundles from a healthy control (**C**) and a patient with CMT1A (**D**). Asterisks mark nerve bundles with myelinated fibres.

the density of bundles without myelinated fibres did not correlate with the dermis area (control: $R = -0.085$, $P = 0.6$, CMT1A: $R = -0.191$, $P = 0.2$; Supplementary Fig. 2B). Since the densities of bundles with myelinated fibres were dependent on the section sizes, we considered this measure not suitable as an outcome for clinical trials.

Mechanoreceptors

Another possible measure to assess the involvement of large myelinated Aβ-fibres in CMT1A is the Meissner corpuscle density. To investigate whether degenerating Meissner corpuscles can be identified by our stains, we searched for Meissner corpuscles that completely lacked either the inner bulb or the enwrapping nerve fibres. Therefore, double staining of the Schwann cells of the inner bulb with anti-S-100 and their enwrapping nerve fibres with PGP9.5 was performed. A total of 235 Meissner corpuscles from 98 samples were examined to identify whether there were Meissner corpuscles that lacked either the inner bulb or the enwrapping nerve fibres. We detected only five Meissner corpuscles in the whole CMT1A cohort that lacked the enwrapping nerve fibres. Next, we determined the Meissner corpuscle density. Patients with CMT1A showed a trend towards decreased Meissner corpuscle density compared with controls (CMT1A–control: $P = 0.064$, Fig. 4A and Table 1). Furthermore, Meissner corpuscle density correlated inversely with age in patients with CMT1A ($R = -0.452$, $P < 0.005$, Fig. 4B). In controls, the negative correlation with age did not reach statistical significance ($R = -0.276$, $P = 0.07$, Fig 4B). We made sure that the number of evaluated papillae did not interfere with the obtained Meissner corpuscle density results. Correlation analyses revealed that there were no correlations between the number of evaluated papillae and the obtained results (control: $R = -0.190$, $P = 0.2$; CMT1A: $R = -0.117$, $P = 0.4$; Supplementary Fig. 3; see Fig. 4C for an intact Meissner corpuscle). Thus, Meissner corpuscle density might be a helpful additional measure in evaluating disease severity.

To further investigate large myelinated nerve fibres, we focused on Merkel cells. Merkel cell density in patients

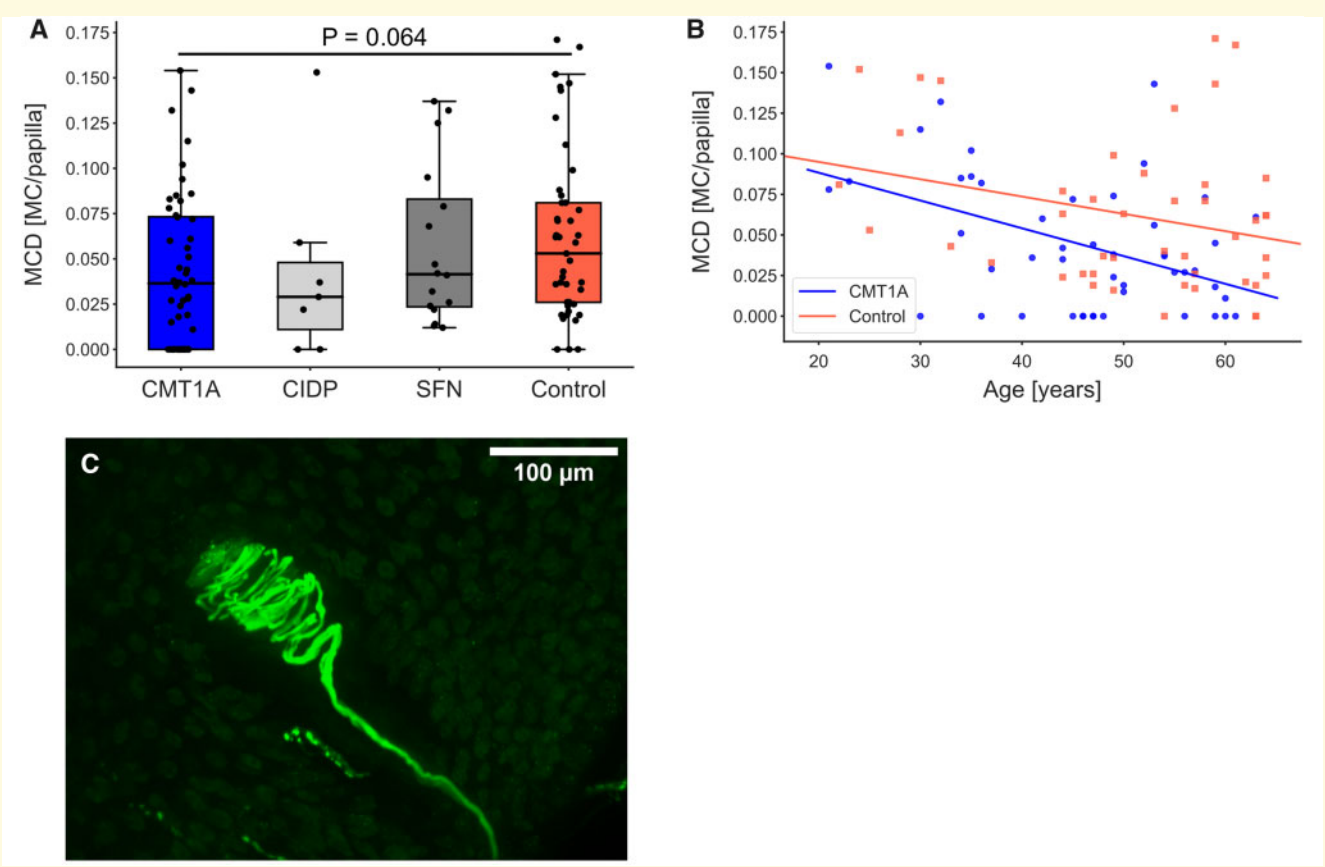

Figure 4 Meissner corpuscle density (MCD) and correlations with age and IENFD. (**A**) Meissner corpuscle density shown as MC per papilla is reduced in CMT1A compared with controls, however not significantly. (**B**) MCD correlates negatively with age in CMT1A ($P < 0.005$, $R = -0.452$), but not in controls ($P = 0.07$, $R = -0.276$). (**C**) Image of Meissner corpuscle in a papilla stained with anti-PGP9.5.

with CMT1A was significantly decreased compared with controls ($P < 0.05$, Fig. 5A and Table 1). Between the other groups, no significant changes were found. Correlation analyses revealed a correlation between Merkel cell density and Meissner corpuscle density in healthy controls ($R = 0.330$, $P < 0.05$), which was not found in the CMT1A group ($R = 0.091$, $P = 0.5$; Fig. 5B).

Since we also observed some denervated Merkel cells, we assumed that these might be degenerating and hence not in contact with nerve fibres. We determined the fraction of denervated Merkel cells of samples showing at least one Merkel cell, which resulted in 39 CMT1A, 5 CIDP, 12 SFN and 40 control samples (Table 1). Comparison of the groups revealed a significant increase in the fraction of denervated Merkel cells in patients with CMT1A compared with the SFN and control groups (Fig. 5C). Moreover, the fraction of denervated Merkel cells correlated with age in the CMT1A group ($R = 0.373$, $P < 0.05$; Fig. 5D; see Fig. 5E and F for examples of sections from a healthy control and a patient with CMT1A stained for Merkel cells and nerve fibres, respectively). Normally innervated Merkel cells in comparison to a denervated Merkel cell are shown in Fig. 5G and H. Correlations between the fraction of denervated Merkel cells and the CMTNSv2 or its subscores could not be detected. In controls, however, the fraction of denervated Merkel cells showed an inverse correlation with Merkel cell density ($R = -0.313$, $P < 0.05$, Supplementary Fig. 4A), which means that Merkel cells in samples with low Merkel cell density tended to be denervated more often than those in samples with higher Merkel cell density. This is consistent with the findings in the CMT1A group, where Merkel cell density is very low and the fraction of denervated Merkel cells is very high. As a methodological control, we ascertained that Merkel cell density did not correlate with the length of analysed epidermis (Supplementary Fig. 4B).

Nodes of Ranvier

Since CMT1A is a demyelinating disease, we investigated the architecture of the nodes of Ranvier in skin sections (Supplementary Fig. 5). A previous study showed a shortened paranodal length in CMT1A biopsies and an increased asymmetry index compared with healthy controls (Saporta *et al.*, 2009).

In all four groups, nodes of Ranvier with comparable axonal diameters were measured as shown in Fig. 6A. In

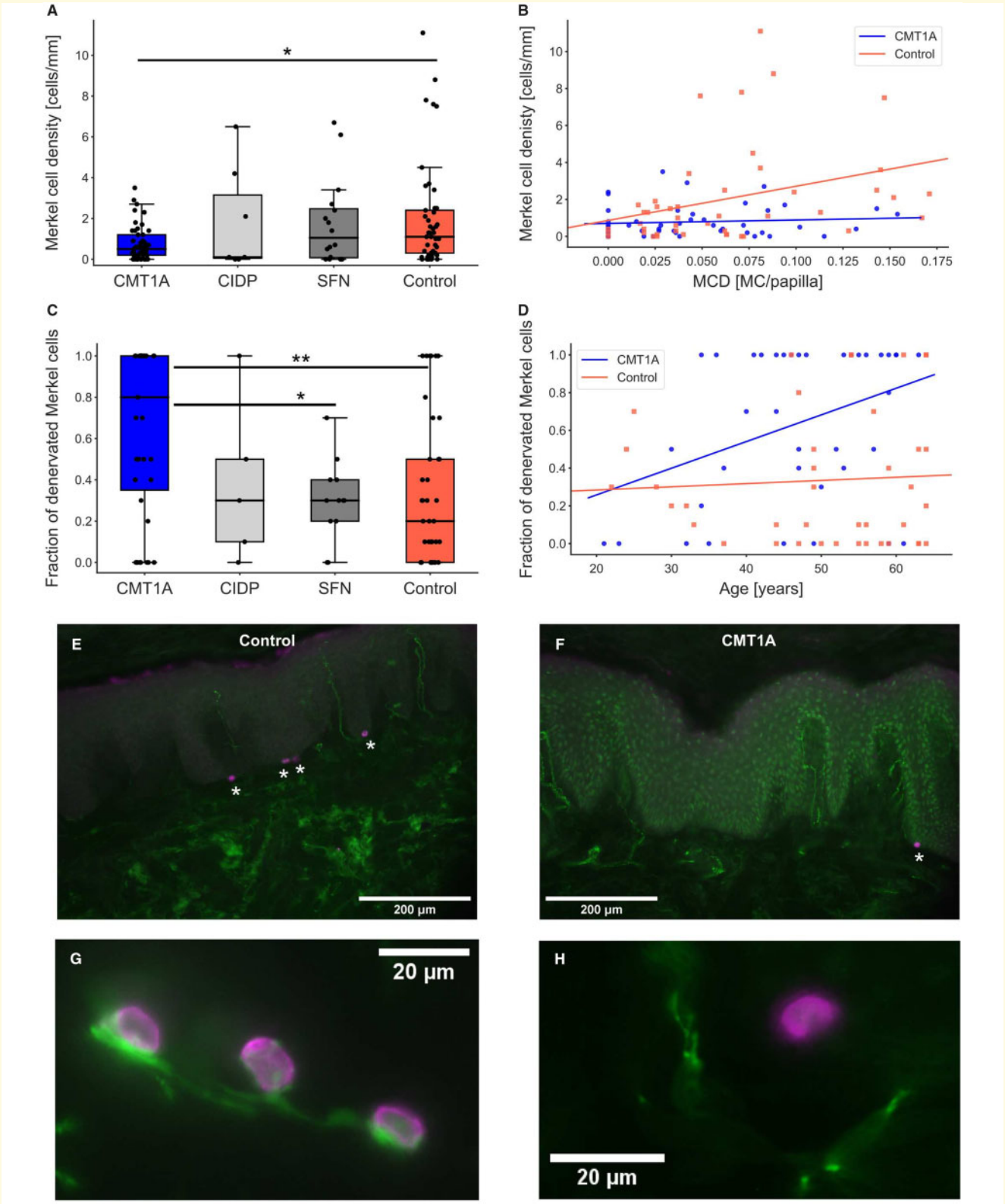

Figure 5 Merkel cell density and fraction of denervated Merkel cells. (**A**) Reduced Merkel cell density in CMT1A compared with healthy controls; *$P < 0.05$. (**B**) Merkel cell density correlated with Meissner corpuscle density (MCD) in controls ($P < 0.05$, $R = 0.330$), but not in patients with CMT1A ($P = 0.5$, $R = 0.091$). (**C**) The fraction of denervated Merkel cells was significantly elevated in CMT1A compared with the SFN and control groups; $P < 0.05$, **$P < 0.01$. (**D**) The fraction of denervated Merkel cells correlated with age in the CMT1A group ($P < 0.05$, $R = 0.373$), but not in the controls ($P = 0.7$, $R = 0.059$). (**E**–**H**) Micrographs of Merkel cells (magenta, anti-CK20) and nerve fibres (green, anti-PGP9.5). Skin sections of a representative healthy control (**E**) and a patient with CMT1A (**F**). Images of innervated Merkel cells (**G**) in comparison to a denervated Merkel cell (**H**) are shown.

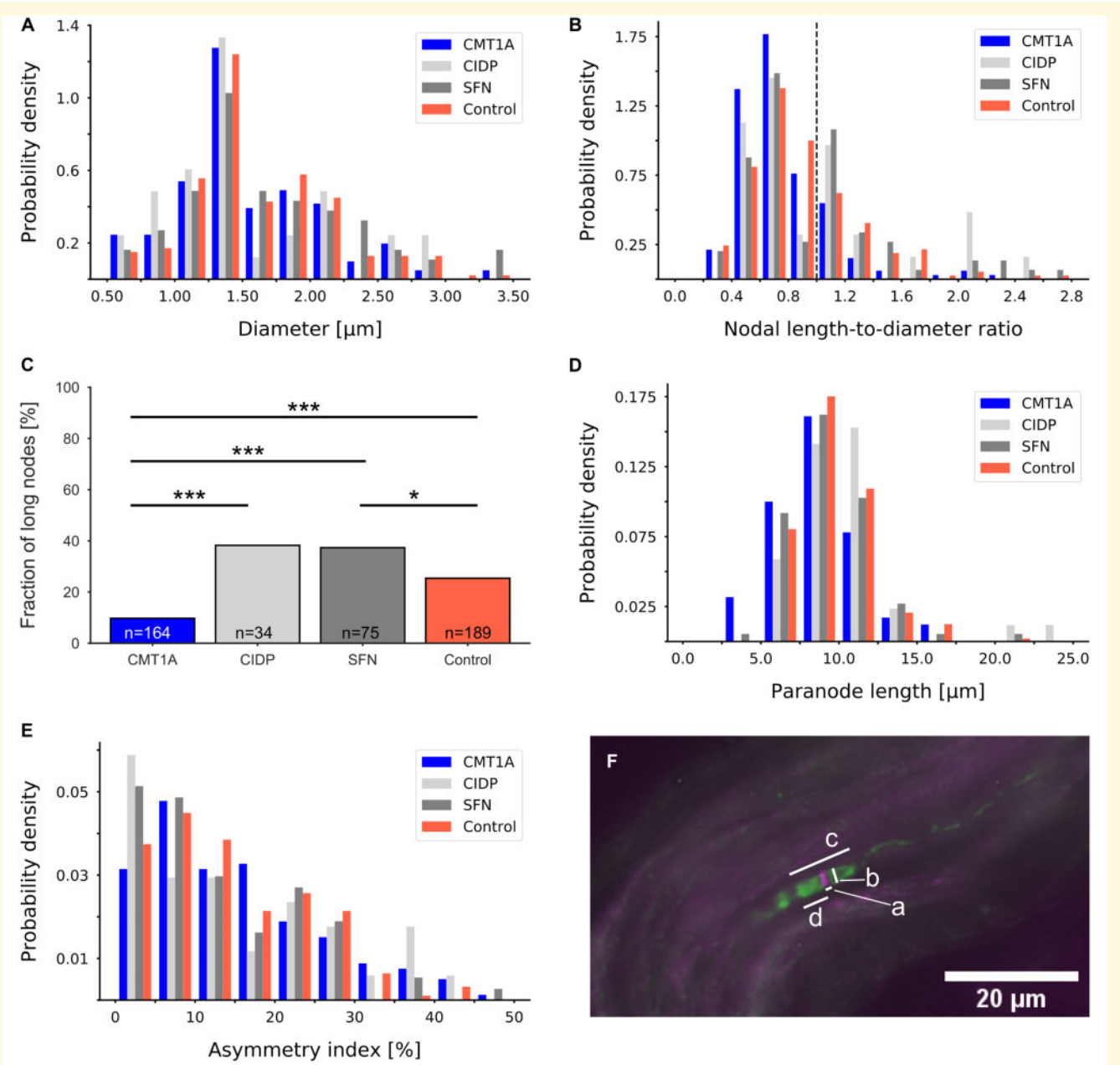

Figure 6 Nodal and paranodal parameters. (**A**) Distributions of axonal diameter of CMT1A, CIDP, SFN and healthy control groups did not show any significant differences. (**B**) Distributions of ratios between the measured nodal gap length and the nodal diameter. Nodes with a ratio of >1 were considered long. The dashed line marks the ratio of 1. There were significantly fewer long nodes in the CMT1A group than in the other groups (CIDP: $P < 0.005$, SFN: $P < 0.001$, control: $P < 0.00001$). (**C**) Fractions of long nodes in the four groups; binomial test; *$P < 0.05$, ***$P < 0.001$. (**D**) Distribution of paranodal lengths. In patients with CMT1A, paranodal length was significantly decreased compared with the CIDP and control groups (CIDP: $P < 0.01$, SFN: $P = 0.08$, control: $P < 0.001$). (**E**) Distributions of asymmetry indices did not differ between the groups. (**F**) Representative micrograph of a node of Ranvier double-labelled with anti-pan-sodium channel (magenta) and anti-Caspr (green). Measurements were taken as indicated: a: nodal length, b: axonal diameter, c: paranodal length, d: length of hemiparanode.

Fig. 6F, a representative micrograph of a node of Ranvier is shown with an indication how the parameters for the analyses were measured. In CMT1A samples, the nodal length-to-diameter ratio was significantly decreased in comparison to all other groups (CIDP: $P < 0.005$, SFN: $P < 0.001$, control: $P < 0.00005$; Fig. 6B), which is also in accordance with the decreased node length in CMT1A (Table 1). Furthermore, the fraction of long nodes was significantly decreased in patients with CMT1A compared with all other groups (Fig. 6C). Similarly, paranodal length of the CMT1A group was significantly decreased compared with the CIDP and

control groups (CIDP: $P < 0.01$, SFN: $P = 0.08$, control: $P < 0.001$, Fig. 6D). Asymmetry indices did not differ between our groups (Fig. 6E). In controls, there was no correlation between age and these nodal parameters. In the CMT1A group, nodal parameters correlated neither with age nor with the CMTNSv2.

Langerhans cells

Langerhans cells are dendritic cells that are located throughout the epidermis (Merad *et al.*, 2008), which makes them a suitable target for investigations of skin biopsies independent of the section depth. Previously, it has been described that Langerhans cell density is decreased in CMT1A compared with controls in skin biopsies from the distal leg (Duchesne *et al.*, 2018).

Langerhans cell density of patients with CMT1A was not different from the control or the SFN groups. In the CIDP group, Langerhans cell density was increased compared with patients with CMT1A and SFN (Fig. 7, both $P < 0.05$). There were no correlations between Langerhans cell density and the length of the analysed section in both the CMT1A group and the control group (Supplementary Fig. 6).

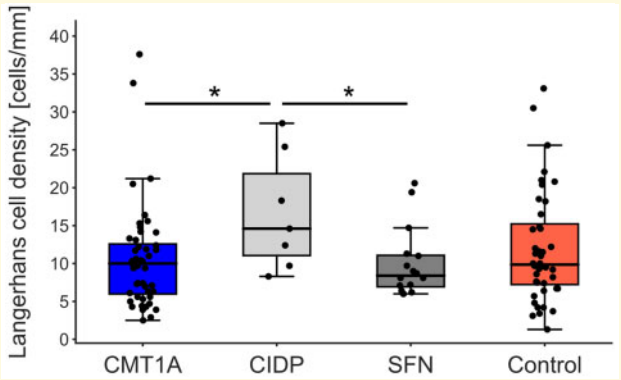

Figure 7 Langerhans cell density was not different in CMT1A compared with SFN or controls. In patients with CIDP, Langerhans cell density was increased compared with patients with CMT1A and SFN; *$P < 0.05$.

Discussion

In our cohort of 48 patients with CMT1A, we investigated a series of candidates for possible outcome measures in CMT1A by the analysis of 3-mm skin punch biopsy sections from the lateral index finger. We identified IENFD, Meissner corpuscle and Merkel cell density as possible outcome measures that assess nerve damage in CMT1A. Thereby, we could show a loss of large and small nerve fibres, the latter correlating with disease severity as assessed by CMTNSv2.

The analysis of IENFD revealed the reduction in small epidermal nerve fibres in CMT1A when compared with healthy controls. A loss of IENFs in CMT1A was previously described in a cohort of 20 biopsies from the fingertip, the thigh and the distal leg (Nolano *et al.*, 2015) and in another study with 75 biopsies from the distal leg (Duchesne *et al.*, 2018). Previous correlation analyses of IENFD in the leg, the thigh and the fingertip revealed a negative correlation with age, but not with the disease severity (Nolano *et al.*, 2015; Duchesne *et al.*, 2018). In our cohort, IENFD did not correlate with age in patients with CMT1A as opposed to our controls but correlated negatively with the disease severity. As to the involvement of small nerve fibres in the demyelinating disease CMT1A, it has been argued that disturbances in axon–Schwann cell interactions in myelinated fibres and in Remak bundles might cause nerve fibre degeneration since also nonmyelinating Schwann cells contain PMP22 in their plasma membranes (Nolano *et al.*, 2015; Duchesne *et al.*, 2018). These results indicate that small nerve fibres decline with increasing CMT1A severity in glabrous skin from the finger. IENFD was independent of the length of the analysed epidermis, which reduces one important factor of potential variability and makes this measure suitable as an outcome measure in clinical trials.

Although nerve bundle densities have been reported to be a good measure for cutaneous innervation in neuropathies, we showed that the density is not independent of the analysed dermis area, which makes it rather difficult to ensure reproducibility compared with the IENFD. Therefore, it is very important to compare data obtained by the analysis of comparable amounts of tissue. This led us to the conclusion that in this study, in which skin samples vary highly in size, this measure is not suitable and reliable.

To be still able to evaluate large myelinated nerve fibres in CMT1A, we examined the densities of mechanoreceptors located at the dermal–epidermal border. There was a reduction in Meissner corpuscles in CMT1A compared with healthy controls, though not significant. In contrast to our control group, the Meissner corpuscle density of patients with CMT1A correlated with age, suggesting that the ongoing deterioration of Meissner corpuscles is accelerated in CMT1A. In fact, Meissner corpuscle density has been previously considered a possible candidate for outcome measures in therapeutic trials for CMT1A (Saporta *et al.*, 2009; Almodovar *et al.*, 2011; Manganelli *et al.*, 2015). Other groups investigating the Meissner corpuscle density, however, only analysed small groups of patients using different techniques or investigating different locations of the hand (Saporta *et al.*, 2009; Almodovar *et al.*, 2011; Manganelli *et al.*, 2015; Nolano *et al.*, 2015). Results of correlation analyses varied between these studies and were not in accordance to our results. A possible reason for the discrepancy between these studies and our data might be the differing units. Since we observed the papillae to vary in size, we decided to not measure the length

of the section but to quantify the Meissner corpuscles in respect to the number of papillae, whereas others provided densities per area.

Although Meissner corpuscles are involved in the perception of vibration (Myers *et al.*, 2013), we could not detect correlation between the Meissner corpuscle density and the vibration subscore. The Meissner corpuscle density is very low and assessed at the finger. The vibration test however is conducted on the feet and legs, which may be one reason for the lack of correlation between these two measures.

We found that the loss of Meissner corpuscles is accelerated by the disease in patients with CMT1A compared with healthy controls, in which the relationship between age and Meissner corpuscle deterioration is not as pronounced as in the patients. Considering these findings, the Meissner corpuscle density might be an additional tool supporting the assessment of the nerve damage and disease severity in CMT1A.

Although a loss of Merkel cells has previously been described in P0-deficient mice (Frei *et al.*, 1999), this measure has not been used in human skin samples to our knowledge. Similar to the Meissner corpuscle density, we could see a reduction in Merkel cells in CMT1A compared with the healthy controls. Furthermore, we noticed that Merkel cells that did not cluster together but were singled out tended to be denervated rather than clustered Merkel cells. Therefore, we determined the fraction of denervated Merkel cells and found highly elevated fractions of denervated Merkel cells in patients with CMT1A compared with controls. This finding suggests that the disease promotes the deterioration of myelinated nerve fibres and therefore Merkel cells. This suggests the density and the ratio of denervated Merkel cells as useful tools for the assessment of nerve damage.

To examine myelinated nerve fibres more carefully, we investigated the architecture of the nodes of Ranvier in nerves throughout the dermis. Although the axon calibres of the investigated nodes of Ranvier were comparable between the groups, we found shortened nodes and paranodes in the CMT1A group. Shortening of paranodes has also been observed in *Trembler-J* mice (Faivre-Sarrailh and Devaux, 2013), which have been considered a rodent model for CMT1A (Faivre-Sarrailh and Devaux, 2013; Nicks *et al.*, 2013). Saporta *et al.* (2009) also described shortening of paranodes and, however, reported a higher asymmetry index compared to controls. A reason for this discrepancy could be the differences in analysis between the two studies. Saporta *et al.* measured every single node they found in the skin sections. We however randomly chose five nodes, if possible, from each sample. Possibly, more symmetric nodes than asymmetric nodes were included in our evaluation leading to this effect. Since the acquisition of the paranodal parameters is very time consuming but presents only weak effects in relation to disease severity, we concluded that this measure is too impracticable for analysis in future studies.

Although Langerhans cell density was reported to be reduced in CMT1A in a previous study (Duchesne *et al.*, 2018), we could not confirm this finding in our cohort. This might be due to the fact that, in the previous study, skin samples from the leg were analysed as opposed to our biopsies from the glabrous part of the index finger. The fact that Langerhans cell density was higher in CIDP, an inflammatory disease, supports the validity of our findings. We concluded that the Langerhans cell density is not a helpful measure in CMT1A when glabrous skin biopsies are used.

Alternative potential biomarkers for CMT1A are under evaluation in other studies. For example, mRNA levels of PMP22 in the skin have been analysed (Katona *et al.*, 2009; Fledrich *et al.*, 2012; Nobbio *et al.*, 2014) and measurements of intramuscular fat by magnetic resonance imaging have been described as possible biomarkers (Morrow *et al.*, 2016; Cornett *et al.*, 2019). In addition, plasma neurofilament light chain concentration has been suggested a biomarker in CMT1A (Sandelius *et al.*, 2018). A short overview of biomarkers evaluating skin and plasma parameters has been prepared by Pareyson and Shy (2018).

One of the limitations of our study might be the relatively few patients in our cohort in the age group from 20 to 30 years since this might have introduced a bias. Another aspect to consider is that our study is cross-sectional and not supported by a longitudinal data acquisition. Furthermore, we have collected skin samples from the lateral part of the index and not the fingertip, which is usually more innervated, to minimize the patients discomfort after the biopsy. Still, we were able to evaluate cutaneous innervation at this biopsy site.

In summary, the measures IENFD and the densities of Meissner corpuscles and Merkel cells appear to be valuable parameters in assessing the disease severity of CMT1A. The paranodal parameters and the Langerhans cell density might be used, since there were no difficulties in assessing them. However, they did not lead to a great gain of knowledge about the disease severity in CMT1A. Nerve bundle density did not prove to be a suitable outcome measure. To confirm the identified measures as useful outcome measures for future clinical trials, follow-up biopsies of the patients need to be assessed to check if they are suitable, not only for the assessment of the disease severity but also for the evaluation of the disease progression in CMT1A.

Supplementary material

Supplementary material is available at *Brain Communications* online.

Acknowledgements

We thank Barbara Dekant for excellent technical assistance. We thank Dr. rer. nat. Lisa Reinecke for excellent

coordination within CMT-NET. Skin biopsy samples were obtained through the German network on Charcot–Marie–Tooth Disease (CMT-NET, service structure S3a, 01GM1511C) funded by the German ministry of education and research (BMBF, Bonn, Germany).

Funding

This study was supported by the German Ministry of Education and Research (BMBF, CMT-NET, 01GM1511F).

Competing interests

The authors report no competing interests.

References

Abraira VE, Ginty DD. The sensory neurons of touch. Neuron 2013; 79: 618–39.

Airaksinen MS, Koltzenburg M, Lewin GR, Masu Y, Helbig C, Wolf E, et al. Specific subtypes of cutaneous mechanoreceptors require neurotrophin-3 following peripheral target innervation. Neuron 1996; 16: 287–95.

Almodovar JL, Ferguson M, McDermott MP, Lewis RA, Shy ME, Herrmann DN. In vivo confocal microscopy of Meissner corpuscles as a novel sensory measure in CMT1A. J Peripher Nerv Syst 2011; 16: 169–74.

Attarian S, Vallat JM, Magy L, Funalot B, Gonnaud PM, Lacour A, et al. An exploratory randomised double-blind and placebo-controlled phase 2 study of a combination of baclofen, naltrexone and sorbitol (PXT3003) in patients with Charcot–Marie–Tooth disease type 1A. Orphanet J Rare Dis 2014; 9: 199–214.

Barreto L, Oliveira FS, Nunes PS, De França Costa IMP, Garcez CA, Goes GM, et al. Epidemiologic study of Charcot–Marie–Tooth disease: a systematic review. Neuroepidemiology 2016; 46: 157–65.

Boulais N, Misery L. Merkel cells. J Am Acad Dermatol 2007; 57: 33–8.

Collongues N, Samama B, Schmidt-Mutter C, Chamard-Witkowski L, Debouverie M, Chanson JB, et al. Quantitative and qualitative normative dataset for intraepidermal nerve fibers using skin biopsy. PLoS One 2018; 13: e0191614.

Cornett KMD, Wojciechowski E, Sman AD, Walker T, Menezes MP, Bray P, et al.; FAST Study Group. Magnetic resonance imaging of the anterior compartment of the lower leg is a biomarker for weakness, disability, and impaired gait in childhood Charcot–Marie–Tooth disease. Muscle Nerve 2019; 59: 213–7.

Doppler K, Stengel H, Appeltshauser L, Grosskreutz J, King Man Ng J, Meinl E, et al. Neurofascin-155 IgM autoantibodies in patients with inflammatory neuropathies. J Neurol Neurosurg Psychiatry 2018; 89: 1145–51.

Doppler K, Werner C, Henneges C, Sommer C. Analysis of myelinated fibers in human skin biopsies of patients with neuropathies. J Neurol 2012; 259: 1879–87.

Doppler K, Werner C, Sommer C. Disruption of nodal architecture in skin biopsies of patients with demyelinating neuropathies. J Peripher Nerv Syst 2013; 18: 168–76.

Duchesne M, Danigo A, Richard L, Vallat JM, Attarian S, Gonnaud PM, et al. Skin biopsy findings in patients with CMT1A: baseline data from the CLN-PXT3003-01 study provide new insights into the pathophysiology of the disorder. J Neuropathol Exp Neurol 2018; 77: 274–81.

Faivre-Sarrailh C, Devaux JJ. Neuro-glial interactions at the nodes of Ranvier: implication in health and diseases. Front Cell Neurosci 2013; 7: 1–13.

Fledrich R, Mannil M, Leha A, Ehbrecht C, Solari A, Pelayo-Negro AL, et al. Biomarkers predict outcome in Charcot–Marie–Tooth disease 1A. J Neurol Neurosurg Psychiatry 2017; 88: 941–52.

Fledrich R, Schlotter-Weigel B, Schnizer TJ, Wichert SP, Stassart RM, Meyer Zu Hörste G, et al. A rat model of Charcot–Marie–Tooth disease 1A recapitulates disease variability and supplies biomarkers of axonal loss in patients. Brain 2012; 135: 72–87.

Frei R, Mötzing S, Kinkelin I, Schachner M, Koltzenburg M, Martini R. Loss of distal axons and sensory Merkel cells and features indicative of muscle denervation in hindlimbs of P0-deficient mice. J Neurosci 1999; 19: 6058–67.

Gess B, Baets J, De Jonghe P, Reilly MM, Pareyson D, Young P. Ascorbic acid for the treatment of Charcot–Marie–Tooth disease. Cochrane Database Syst Rev 2015; CD011952.

Gess B, Schirmacher A, Boentert M, Young P. Charcot–Marie–Tooth disease: frequency of genetic subtypes in a German neuromuscular center population. Neuromuscul Disord 2013; 23: 647–51.

Gøransson LG, Mellgren SI, Lindal S, Omdal R. The effect of age and gender on epidermal nerve fiber density. Neurology 2004; 62: 774–7.

Katona I, Wu X, Feely SME, Sottile S, Siskind CE, Miller LJ, et al. PMP22 expression in dermal nerve myelin from patients with CMT1A. Brain 2009; 132: 1734–40.

Lauria G, Cornblath DR, Johansson O, McArthur JC, Mellgren SI, Nolano M, et al. EFNS guidelines on the use of skin biopsy in the diagnosis of peripheral neuropathy. Eur J Neurol 2005; 12: 747–58.

Lauria G, Lombardi R, Camozzi F, Devigili G. Skin biopsy for the diagnosis of peripheral neuropathy. Histopathology 2009; 54: 273–85.

Lee S, Bazick H, Chittoor-Vinod V, Al Salihi MO, Xia G, Notterpek L. Elevated peripheral myelin protein 22, reduced mitotic potential, and proteasome impairment in dermal fibroblasts from Charcot–Marie–Tooth disease type 1A patients. Am J Pathol 2018; 188: 728–38.

Lewis RA, McDermott MP, Herrmann DN, Hoke A, Clawson LL, Siskind C, et al. High-dosage ascorbic acid treatment in Charcot–Marie–Tooth disease type 1A results of a randomized, double-masked, controlled trial. JAMA Neurol 2013; 70: 981–7.

Li J, Bai Y, Ghandour K, Qin P, Grandis M, Trostinskaia A, et al. Skin biopsies in myelin-related neuropathies: bringing molecular pathology to the bedside. Brain 2005; 128: 1168–77.

Li J, Parker B, Martyn C, Natarajan C, Guo J. The PMP22 gene and its related diseases. Mol Neurobiol 2013; 47: 673–98.

Manganelli F, Nolano M, Pisciotta C, Provitera V, Fabrizi GM, Cavallaro T, et al. Charcot–Marie–Tooth disease: new insights from skin biopsy. Neurology 2015; 85: 1202–8.

Manganelli F, Tozza S, Pisciotta C, Bellone E, Iodice R, Nolano M, et al. Charcot–Marie–Tooth disease: frequency of genetic subtypes in a Southern Italy population. J Peripher Nerv Syst 2014; 19: 292–8.

Mannil M, Solari A, Leha A, Pelayo-Negro AL, Berciano J, Schlotter-Weigel B, et al. Selected items from the Charcot–Marie–Tooth (CMT) neuropathy score and secondary clinical outcome measures serve as sensitive clinical markers of disease severity in CMT1A patients. Neuromuscul Disord 2014; 24: 1003–17.

Merad M, Ginhoux F, Collin M. Origin, homeostasis and function of Langerhans cells and other langerin-expressing dendritic cells. Nat Rev Immunol 2008; 8: 935–47.

Micallef J, Attarian S, Dubourg O, Gonnaud P-M, Hogrel J-Y, Stojkovic T, et al. Effect of ascorbic acid in patients with Charcot–Marie–Tooth disease type 1A: a multicentre, randomised, double-blind, placebo-controlled trial. Lancet Neurol 2009; 8: 1103–10.

Morrow JM, Sinclair CDJ, Fischmann A, Machado PM, Reilly MM, Yousry TA, et al. MRI biomarker assessment of neuromuscular disease progression: a prospective observational cohort study. Lancet Neurol 2016; 15: 65–77.

Murphy SM, Herrmann DN, McDermott MP, Scherer SS, Shy ME, Reilly MM, et al. Reliability of the CMT neuropathy score (second version) in Charcot–Marie–Tooth disease. J Peripher Nerv Syst 2011; 16: 191–8.

Myers MI, Peltier AC, Li J. Evaluating dermal myelinated nerve fibers in skin biopsy. Muscle Nerve 2013; 47: 1–11.

Nicks JR, Lee S, Kostamo KA, Harris AB, Sookdeo AM, Notterpek L. Long-term analyses of innervation and neuromuscular integrity in the trembler-J mouse model of Charcot–Marie–Tooth disease. J Neuropathol Exp Neurol 2013; 72: 942–54.

Nobbio L, Visigalli D, Radice D, Fiorina E, Solari A, Lauria G, et al.; CMT-TRIAAL Group. PMP22 messenger RNA levels in skin biopsies: testing the effectiveness of a Charcot–Marie–Tooth 1A biomarker. Brain 2014; 137: 1614–20.

Nolano M, Manganelli F, Provitera V, Pisciotta C, Stancanelli A, Caporaso G, et al. Small nerve fiber involvement in CMT1A. Neurology 2015; 84: 407–14.

Van Paassen BW, Van Der Kooi AJ, Van Spaendonck-Zwarts KY, Verhamme C, Baas F, De Visser M. PMP22 related neuropathies: Charcot–Marie–Tooth disease type 1A and hereditary neuropathy with liability to pressure palsies. Orphanet J Rare Dis 2014; 9: 38–53.

Pareyson D, Reilly MM, Schenone A, Fabrizi GM, Cavallaro T, Santoro L, et al. Ascorbic acid in Charcot–Marie–Tooth disease type 1A (CMTTRIAAL and CMT-TRAUK): a double-blind randomised trial. Lancet Neurol 2011; 10: 320–8.

Pareyson D, Scaioli V, Laurà M. Clinical and electrophysiological aspects of Charcot–Marie–Tooth disease. Neuromolecular Med 2006; 8: 3–22.

Pareyson D, Shy ME. Neurofilament light, biomarkers, and Charcot–Marie–Tooth disease. Neurology 2018; 90: 257–9.

Reilly MM, Shy ME, Muntoni F, Pareyson D. 168th ENMC International Workshop: outcome measures and clinical trials in Charcot–Marie–Tooth disease (CMT). Neuromuscul Disord 2010; 20: 839–46.

Sandelius Å, Zetterberg H, Blennow K, Adiutori R, Malaspina A, Laura M, et al. Plasma neurofilament light chain concentration in the inherited peripheral neuropathies. Neurology 2018; 90: e518–24.

Saporta MA, Katona I, Lewis RA, Masse S, Shy ME, Li J. Shortened internodal length of dermal myelinated nerve fibres in Charcot–Marie–Tooth disease type 1A. Brain 2009; 132: 3263–73.

Snipes GJ, Suter U. Molecular anatomy and genetics of myelin proteins in the peripheral nervous system. J Anat 1995; 186: 483–94.

Sommer C. Skin biopsy as a diagnostic tool. Curr Opin Neurol 2008; 21: 563–8.

Sommer C. Nerve and skin biopsy in neuropathies. Curr Opin Neurol 2018; 31: 534–40.

Üçeyler N, Vollert J, Broll B, Riediger N, Langjahr M, Saffer N, et al. Sensory profiles and skin innervation of patients with painful and painless neuropathies. Pain 2018; 159: 1867–76.

Wang W, Guedj M, Bertrand V, Foucquier J, Jouve E, Commenges D, et al. A Rasch analysis of the Charcot–Marie–Tooth neuropathy score (CMTNS) in a cohort of Charcot–Marie–Tooth type 1A patients. PLoS One 2017; 1: e0169878.